Antibacterial activity of a porous silver doped TiO_2 coating on titanium substrates synthesized by plasma electrolytic oxidation

Monica Thukkaram[1], Pieter Cools[1], Anton Nikiforov[1], Petra Rigole[2], Tom Coenye[2], Pascal Van Der Voort[3], Gijs Du Laing[4], Chris Vercruysse[5], Heidi Declercq[5], Rino Morent[1], Lieven De Wilde[6], De Baets Patrick[7], Kim Verbeken[8], Nathalie De Geyter[1]

[1]Research Unit Plasma Technology (RUPT), Department of Applied Physics, Faculty of Engineering and Architecture, Ghent University, Belgium

[2]Laboratory of Pharmaceutical Microbiology, Faculty of Pharmaceutical Sciences, Ghent University, Belgium

[3]Centre for Ordered Materials, Organometallics and Catalysis (COMOC), Department of Chemistry, Faculty of Sciences, Ghent University, Belgium

[4]Department of Applied and Analytical Chemistry, Faculty of Bioscience Engineering, Ghent University, Belgium

[5]Tissue Engineering Group, Department of Human Structure and Repair, Faculty of Medicine and Health Sciences, Ghent University, Ghent, Belgium

[6]Orthopedic Surgery and Traumatology, Department of Human Structure and Repair, Faculty of Medicine and Health Sciences, Ghent University, Ghent, Belgium

[7]Department of Electrical Energy, Metals, Mechanical Constructions and Systems, Soete Lab, Ghent University, Belgium

[8]Department of Materials, Textiles and Chemical Engineering, Faculty of Engineering and Architecture, Ghent University, Belgium

Abstract

The objective of this study was the development of Ag-rich antibacterial coatings on titanium (Ti) to prevent post-operative infections. A series of Ag-doped TiO_2 coatings were synthesized on Ti discs by plasma electrolytic oxidation (PEO) in an electrolyte containing Ag nanoparticles (AgNPs). The incorporation, distribution and chemical composition of the AgNPs on Ti were determined using scanning electron microscopy-energy dispersive spectroscopy (SEM-EDS). The crystalline structure and wettability of the coating was characterized by X-ray diffraction (XRD) and water contact angle (WCA) analysis respectively. Surface roughness and hardness of the coating were examined using atomic force microscopy (AFM) and Knoop indentation test respectively, while silver ion release was quantified using inductively coupled plasma-mass spectroscopy (ICP-MS).

Following PEO, the surface of the Ti substrate was converted to TiO_2 composed of anatase and rutile phases. The SEM micrographs showed that the AgNPs were distributed throughout the oxide layer, without changing the morphology of the coating. The coatings also revealed an increased surface roughness, enhanced surface microhardness and improved surface wettability relative to untreated Ti substrates. Furthermore, the incorporation of Ag into the coating did not alter the phase component, surface roughness, microhardness and wettability. A series of *in-vitro* antibacterial assays indicated that increasing the number of AgNPs in the electrolyte led to excellent antibacterial activities, resulting in a complete reduction of *Escherichia coli* and a 6-log reduction of *Staphylococcus aureus* after 24 hours of incubation.

Keywords: PEO; Ag-doped TiO_2; Anatase TiO_2; Rutile TiO_2; Antibacterial coating

Graphical abstract

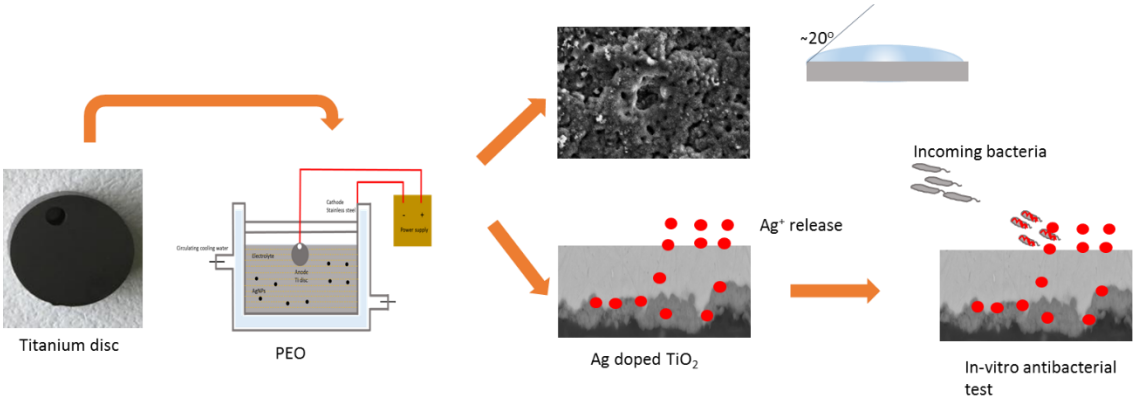

Highlights

- Ag-free and Ag-doped TiO_2 were fabricated on commercially pure titanium by PEO.
- The silver wt% on the coating increases with increasing concentration of AgNPs in the electrolyte.
- PEO coatings exhibited increased surface micro hardness, roughness and wettability in relative to untreated Ti.
- Dose-dependent effect of Ag-doped TiO_2 on antibacterial activity was observed

1. Introduction

Every year more than 1000 tons of titanium (Ti)-based devices of every description and function are implanted in patients. Ti and its alloys are most commonly used for orthopedic implants including bone and joint replacements, fracture fixation devices and dental implants due to their favorable mechanical properties, stability and biocompatibility [1]. Even though Ti implants are expected to last for at least

a decade or more, they often fail prematurely, resulting in revision surgery that is usually characterized by a higher level of complexity and that forms a heavy burden on the current healthcare systems [2,3].

The reasons for implant failure are varying in nature, with bacterial infections on the implant surface being one of the prime reasons. Risk of bacterial infection is high, especially for fracture fixation devices where open fractured bones are involved [4,5]. Once an infection settles, it is a challenging task to treat it and, more often than not, it leads to premature implant removal. In more severe cases, the infection expands to the surrounding tissues or blood stream, which could lead to amputation or mortality. Implant associated infections are the result of bacterial adhesion to an implant surface and subsequent biofilm formation at the implantation site. The biofilm formation takes place in several stages, starting with rapid surface attachment, followed by multi-layered bacterial proliferation and intracellular adhesion in an extracellular polysaccharide matrix. Due to the presence of biofilms, a chronic inflammatory response may develop at the infection site, as treatment with antibiotics is often unsuccessful in removing the biofilm-associated bacteria [6–8].

Therefore, inhibiting initial bacterial adhesion is essential to prevent implant-associated infections. Several strategies of loading antibacterial agents onto implant surfaces have been studied. Compared to the organic antibacterial agents such as chlorhexidine, collagen, chloroxylenol and poly (hexamethylenebiguanide) [9–12], inorganic antibacterial metallic nanoparticles like Ag [13–15], Cu [16–18] and Zn [19–21] have attracted more attention due to their larger surface area to volume ratio, wide therapeutic window, good stability, low risk of producing resistant strains and comparatively low toxicity to human cells [22,23]. Among the inorganic antibacterial metallic nanoparticles, silver nanoparticles (AgNPs) are by far the most widely examined due to the non-toxicity of the active Ag^+ to human cells and their excellent antibacterial activity [24]. It has been demonstrated that Ag^+ can interact with bacterial cells, leading to an increase in membrane permeability, degradation of lipopolysaccharide molecules, causing damage to the bacterial outer membrane [25]. *In vitro* studies have demonstrated good biocompatibility of silver ion implanted stainless steel coatings without any cytotoxic effect [26] while *in vivo* studies have indicated that Ag^+ containing cobalt chromium coatings have no local or systemic side effect [27].

Surface engineering technologies that can successfully deposit nanoparticle-containing coatings include plasma-assisted physical or chemical vapour deposition [28], ion implantation surface oxidation [19,29], ion beam-assisted deposition [30], magnetron sputtering [31,32] and plasma electrolytic oxidation (PEO) [2,33–35]. Among these techniques, plasma electrolytic oxidation is one of the most versatile and cost-effective ways to modify the surface of metallic implants with complex geometries. PEO is primarily used for aluminium and its alloys, while more recently it has also been

found suitable for the oxidation of magnesium and its alloys [36], titanium and its alloys [2,34], niobium, zirconium and tantalum [37,38]. The coatings fabricated on aluminium alloys have been found to exhibit superior anti-corrosion and mechanical properties, making it suitable for industrial applications [39,40].

PEO-based coatings of Ti and Ti alloys have been of particular interest for the improvement of their tribological properties and biocompatibility and a large variety of PEO-based coatings on Ti substrates has already been investigated [33,41]. During PEO, Ti acts as an anode and is exposed to an electrolyte at an applied high voltage. When the applied voltage is less than the breakdown voltage, an amorphous oxide layer is deposited, whereas when the voltage is higher than the breakdown voltage, the process tends to produce plasma spark discharges leading to the formation of an irregular porous oxide layer, which thickens a native passivating titanium dioxide (TiO_2) layer. The porosity of the anodized film is known to enhance the anchorage of implants and to stimulate the release of antibacterial agents from the titanium implants into its surrounding [42,43]. As such, the bioactivity and antibacterial properties of the coating can be tuned by controlling the applied voltage, electrolyte composition, treatment time, and current density. Recent studies have shown the feasibility of the PEO process for the synthesis of antibacterial coatings on Ti alloys using electrolytes bearing Ag/Cu NPs [44,45]. Furthermore, *in-vitro* antibacterial activity of the coatings against gram-positive bacteria was also demonstrated via direct contact assays. However, the influence of electrolyte composition on the properties of the coatings and a comprehensive scanning electron microscopical study of the PEO coatings in the presence of AgNPs have not been addressed sufficiently so far.

The aims of this particular study are therefore: (i) the synthesis of porous TiO_2 coatings on Ti substrates with and without bearing AgNPs by plasma electrolytic oxidation; (ii) the assessment of the physical and chemical characteristics of the deposited coatings using different characterization techniques such as scanning electron microscopy-energy dispersive spectroscopy (SEM/EDS), X-ray diffraction (XRD), water contact angle (WCA) analysis, atomic force microscopy (AFM) and hardness tests and (iii) evaluation of the silver ion release kinetics and the *in-vitro* antibacterial activity of the coatings against *E. coli* (Gram-negative bacterium) and *S. aureus* (Gram-positive bacterium).

2. Materials and Methods

2.1 Preparation of Ti specimens

Commercially used pure titanium discs (diameter: 12 mm and thickness: 3 mm) purchased from L&D Techniek NV were used as substrates. AgNPs with an average diameter of 50 nm were purchased from Sigma-Aldrich and used as such. Prior to the PEO treatment, Ti samples were ground with SiC paper up

to 1200 and mirror-like polished after which they were ultrasonically cleaned with acetone, ethanol and distilled water.

2.2 Preparation of PEO coatings

The experimental set-up used to perform the PEO process is schematically represented in fig. 1. The PEO process was performed at a fixed DC voltage of 400 V for 5 min in an electrolyte cell containing 150 ml of the electrolyte. The working electrolyte was 0.4 g/L NaOH and 4.0 g/L NaH_2PO_4 with and without the addition of AgNPs (concentrations of 0.1 g/L, 0.5 g/L and 1.0 g/L) in 1L of distilled water. The temperature of the electrolyte was kept at 25 ± 5° C by using a water-cooling system during the treatment process to prevent chemical dissolution of the coating. After the treatment, samples were washed with distilled water and air dried. Samples oxidized in the Ag-free electrolyte and the Ag-doped electrolyte containing 0.1 g/L, 0.5 g/L and 1 g/L will be referred to as the TiO_2, Ag1, Ag2 and Ag3 samples, respectively.

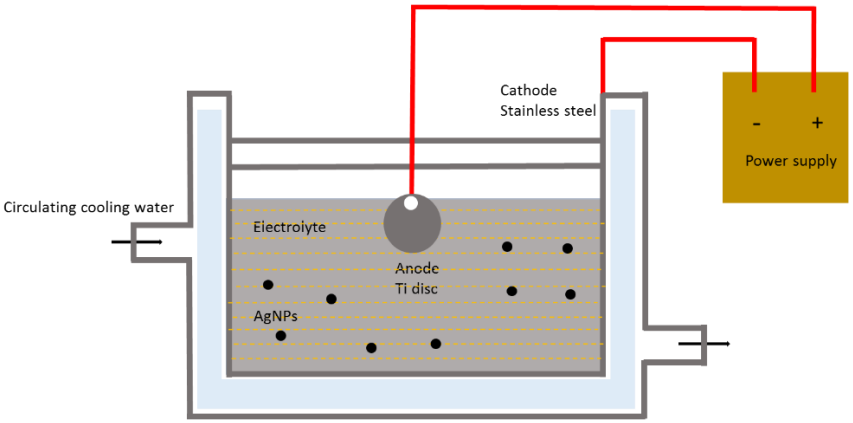

Fig. 1. Schematic diagram of the PEO experimental device.

2.2 SEM-EDS analysis

The surface morphology of the oxidized films was analyzed using a JEOL JSM-6010 PLUS/LV SEM device operated at an accelerating voltage of 7 kV and a working distance of 11 mm. The cross sectional morphology of the oxidized films was analyzed using a JEOL JSM-7600F field emission gun (FEG)-SEM device operating at an accelerating voltage of 15 kV and a working distance of 8 mm. In addition, the elemental composition and elemental mapping of the coatings (surface and cross-sections) were also investigated with an energy dispersive spectrometer (EDS) present on the JSM-7600F FEG-SEM device. 2 samples were analyzed for each condition using both microscopes.

2.3 WCA evaluation

After performing the PEO processes, WCA values of the coated Ti substrates were obtained at room temperature using a commercial Krüss Easy Drop optical system. Distilled water drops of 1 µl were used as test liquid and the WCA values were obtained using Laplace-Young curve fitting. An average WCA value was calculated based on WCA analysis of 3 different samples (2 water drops per sample).

2.4 AFM analysis

Changes in Ti surface topography were quantified using an XE-70 AFM system (Park Systems). Micrographs measuring a surface area of 15 × 15 µm² were recorded in non-contact mode using a silicon-based cantilever (Nanosensors™ PPP-NCHR). The obtained micrographs were analyzed using the included XEP processing software (V1.8.0) and were subjected to an X-Y plane autofit procedure prior to roughness determination. The roughness was characterized by the average roughness (R_a) value, which is defined as the mean of the deviations of the surface height from the median line. In this study, for each sample, measurements were done on five random locations and the sample roughness given is the average of the five obtained values.

2.5 Hardness test

The surface microhardness was evaluated by means of a Shimadzu HMV-2000 microhardness tester equipped with a Knoop indenter at a load of 25 g to 100 g using a fixed loading duration of 10 s. For each sample, the test was performed at ten different locations randomly distributed over the surface from which an average HK value per sample was determined.

2.6 XRD analysis

The crystalline structure of the TiO_2 layers deposited on Ti substrates was studied using a powder X-ray diffraction ARL X'TRA diffractometer (Thermo Scientific) equipped with a Cu Kα (λ = 1.5405 Å) source and operating at angles in the range of 20-80°. The integration time and scan rate were fixed at 1.2 s and 1° min^{-1} respectively. Analysis of the obtained XRD spectra was performed using the American mineralogist crystal structure database.

2.7 Examination of the silver ion release by inductively coupled plasma-mass spectroscopy (ICP-MS)

The silver ion release kinetics of the coatings were monitored by means of a NexION 350 ICP-MS (PerkinElmer) device. Prior to ICP-MS analysis, the Ag-doped TiO_2 coated discs were immersed into 20 ml of distilled water in small glass bottles at room temperature for different time points (3 h, 1 day, 3 days, 5 days and 7 days). In a next step, the concentration of released Ag^+ in the distilled water was determined using ICP-MS. Each reported Ag^+ concentration value is the average of 2 independent measurements.

2.8 *In vitro* antibacterial assay

E. coli ATCC 25922 and *S. aureus* ATCC 6538 were grown on Luria-Bertani (LB) agar or in LB broth at 37°C. An overnight culture was standardized to an optical density (at 590 nm) of 0.05 and subsequently diluted 1:1000 in 2% LB broth. 2 ml of the resulting suspension was added to the wells of a 12-well microtiter plate, each well containing one coated Ti sample. Microtiter plates were subsequently incubated at 37°C for 24 h, with shaking (100 rpm). After 24 h, samples were removed from the microtiter plates and placed in 10 ml physiological saline (0.9% NaCl) after which they were vortexed and sonicated in order to remove all surface-attached bacteria from the samples. Serial dilutions of the resulting suspension were used to determine the number of colony forming units (CFU) by plating on LB agar. 100 µl of the undiluted suspension was at the same time mixed with 10 µl resazurin (CellTiter Blue, Promega), incubated at 37°C for 30 min and the resulting fluorescence (λex 535 nm/λem 590 nm) was measured using a multilabel microtiter plate reader (Envision; PerkinElmer). Experiments were performed on 4 independent samples (n=4) and the obtained data are represented as a mean with standard deviation. For statistical analysis, ANOVA was performed followed by a Tukey's HSD post hoc test and a p-value <0.05 was considered to be significant.

3. Results and discussion

3.1 Coating morphology and distribution of AgNPs

The top surface morphologies of Ag-free (TiO_2) and Ag-doped (Ag1, Ag2 and Ag3) coatings at 1000x and 10000x magnification and their corresponding EDS spectra can be seen in fig. 2(a), (b) and (c) respectively. It was observed that the surfaces of all coatings under investigation exhibited a microporous morphology and that the pores were homogenously distributed over the entire coating surface. Additionally, no obvious differences could be seen in the top surface morphology between the Ag-free sample on the one hand and all Ag-doped samples (Ag1, Ag2 and Ag3) on the other hand. This indicated that the incorporation of AgNPs had no significant effect on the top surface morphology of the coating and that in fact AgNP incorporation did not alter the main structural characteristics including porous morphology and distribution of pores. Similar findings were also observed when using different electrolyte concentrations [46,47]. EDS spot analysis also confirmed that no Ag was found on the Ag-free coating while it was present in all three Ag-doped coatings along with Ti and O from the metallic TiO_2 coating, P from the electrolyte and some small amount of C due to surface contamination (Fig. 2(c)). EDS analysis also showed that the incorporation of Ag in the coating increased from 0.6 wt% to 3.1 wt% as the concentration of AgNPs in the electrolyte increased from 0.1 g/L to 1 g/L (see Table 1). It could also be noted that with increasing concentrations of AgNPs in the alkaline phosphate

electrolyte, the amount of Ti in the surface layer decreased, whereas an increase in phosphorus content and a constant content of oxygen was observed.

To further investigate the distribution of AgNPs on the coating surface, high resolution SEM images in back scattered electron (BSE) mode were also taken for the Ag-doped samples (Ag1, Ag2 and Ag3) at 1000x and 30000x magnification and the results are presented in fig. 3(a) and (b). High atomic number elements (such as Ag) backscatter electrons more strongly than low atomic number elements such as Ti, O, and P and thus appear brighter in BSE micrographs. At low magnification (fig. 3(a)), it can be observed that for all Ag-doped samples AgNPs were mainly distributed as clusters of nanoparticles while some stand-alone nanoparticles within the TiO_2 matrix could also be observed. Fig. 3(a) also reveals that the clustering of the AgNPs increased with increasing concentration of AgNPs in the electrolyte. SEM-BSE images at high magnification (fig. 3(b)) also showed that AgNPs were found to be not only fused on the top surface of the TiO_2 coatings, but also inside the pores of the coating (indicated with the arrow marks). Again, also in fig. 3(b), more AgNPs can be seen when adding higher amounts of AgNPs to the electrolyte.

NPs are incorporated into the growing oxide layer when they are added in the PEO electrolyte. Studies have reported the mechanism of incorporation of NPs within the porous TiO_2 matrix during the PEO process [2,48–50]. These authors stated that different stages are involved in the incorporation of Ag nanoparticles within the porous oxide layer such as the delivery of particles to the sites of oxide matrix, accumulation of particles at the sites of the oxide matrix and preservation of the already embedded particles during coating growth. Many studies have also investigated the incorporation of nanoparticles like Ag, Cu and Zn within a TiO_2 matrix [21]. These authors have reported that the nanoparticles are delivered into the oxide coating via transport pathways such as pores, cracks and short-circuit channels. Then, these particles are embedded at the sites of coating growth which are preserved during the growth of the oxide layer [2,51].

Fig. 4 shows the cross-sectional SEM-BSE micrographs of the Ag-free (TiO_2) and the Ag-doped coatings (Ag1, Ag2 and Ag3) and their corresponding elemental mapping of Ti, O, P and Ag. Based on these cross-sectional images, the thicknesses of the oxide layers were measured as 4.7 ± 0.5 µm, 5.5 ± 1.1 µm, 5.1 ± 0.6 µm and 5.9 ± 1.9 µm for the TiO_2, Ag1, Ag2 and Ag3 samples respectively. Consequently, adding different amounts of AgNPs to the electrolyte did not affect the final thickness of the created oxide layer. From the EDS elemental mapping, it can also be observed that Ti, O and P were uniformly distributed along the coating surface and coating thickness. From the Ag mapping results it also became apparent that the AgNPs preferably aggregated at the O and P layer in case of the Ag2 and Ag3 samples.

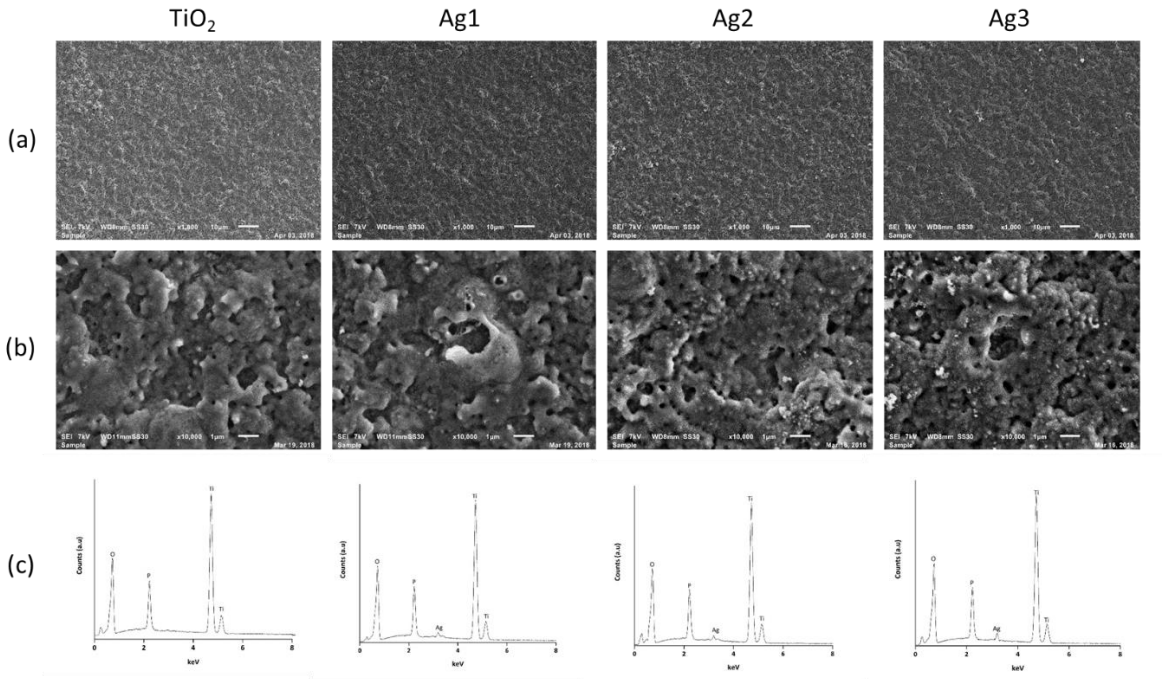

Fig. 2. Surface SEM micrographs of Ag-free (TiO_2) and Ag-doped (Ag1, Ag2, Ag3) TiO_2 coatings at 1000x magnification (a) and 10,000x magnification (b) and their corresponding EDS spectra (c).

Table 1. Elemental composition of Ag-free and Ag-doped TiO_2 coatings obtained from EDS analysis.

Coated Surface	**Ti (wt%)**	**O(wt%)**	**P (wt%)**	**Ag (wt%)**
TiO_2	53.7 ± 2.1	41.1 ± 1.3	5.2 ± 2.4	0
Ag1	49.5 ± 2.5	42.5 ± 2.7	6.4 ± 0.1	0.6 ± 0.4
Ag2	48.4 ± 1.9	43.2 ± 1.8	6.9 ± 0.2	1.2 ± 0.2
Ag3	47.1 ± 1.6	42.3 ± 0.9	6.8 ± 0.2	3.1 ± 0.2

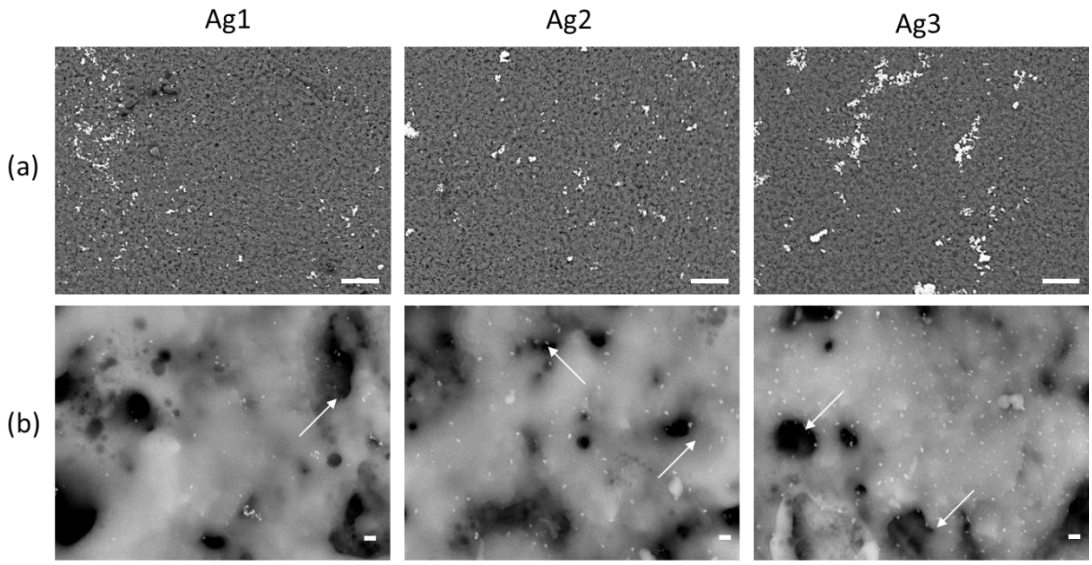

Fig. 3. SEM-BSE images of the surface of antibacterial coatings (Ag1, Ag2, Ag3) at 1000x magnification (a) and 30000x magnification (b) clearly showing the presence of AgNPs (scale bar: 10 µm (a) and 100 nm (b)). The arrows indicate the incorporation of AgNPs inside the coating pores.

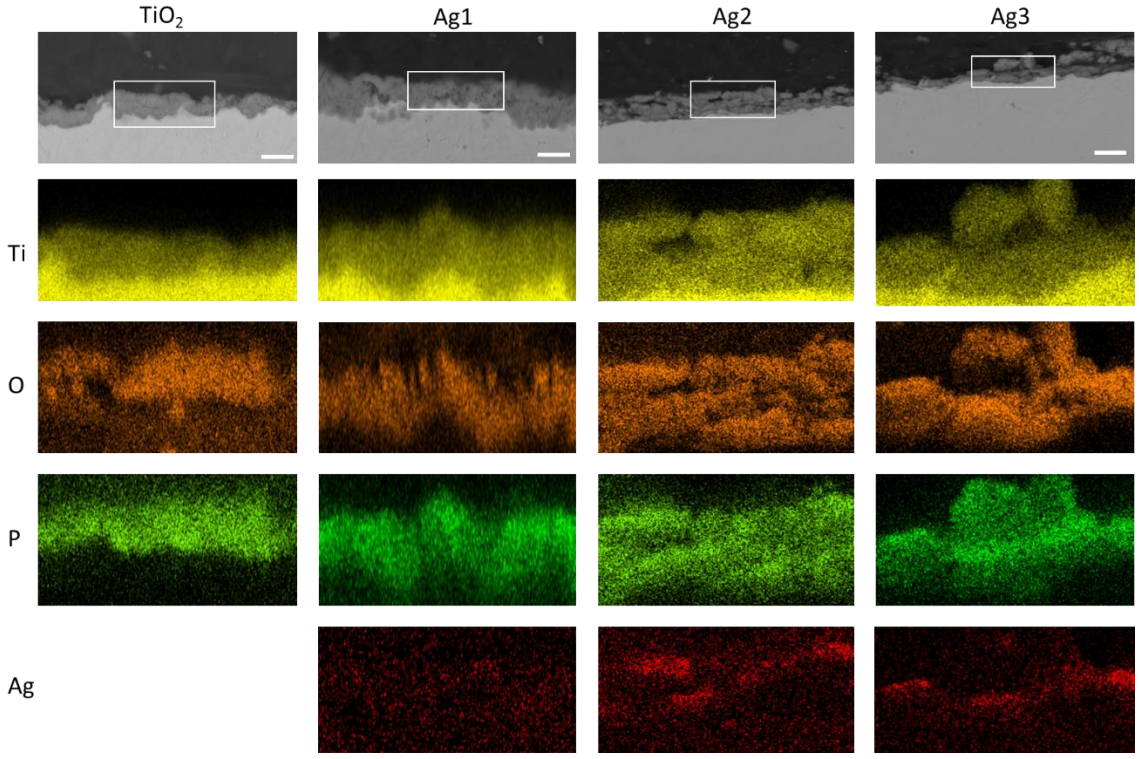

Fig. 4. Cross-sectional SEM-BSE images and EDS mapping corresponding to the framed area in the upper SEM-BSE images of the TiO_2, Ag1, Ag2 and Ag3 coatings (Scale bar: 5 µm).

3.2 Surface crystallinity

Fig. 5 shows the X-ray diffraction patterns of untreated Ti, the Ag-free and different Ag-doped TiO_2 coated Ti substrates. The untreated Ti sample consisted of both the pure Ti phase as well as very small amounts of oxidized titanium phases, which were identified as anatase and rutile TiO_2. As can be seen in fig. 5, after performing the PEO processes, the peak intensities of these anatase and rutile TiO_2 phases strongly increased compared to the untreated Ti sample while the intensity of the Ti peaks decreased. Nevertheless, Ti peaks were still present on the XRD spectra of the PEO treated samples due to the penetration of the X-ray beam beyond the TiO_2 coating. In addition, there were no obvious differences in crystalline phases between the Ag-free TiO_2 coatings and the TiO_2 coatings doped with different amounts of AgNPs. This observation is in contrast with the results reported in another study, where the presence of Ag diffraction peaks was observed for Ag-doped coatings [44]. This difference could be attributed to the different method of incorporating silver into the coating or due to the low amount of AgNPs incorporated in the coatings fabricated in this work resulting in a total silver content below the detection limit of the XRD system.

It should be noted that TiO_2 exists in three different crystal lattices: anatase, rutile and brookite. After PEO treatment, the thickness of the oxide layer increased to approximately 5 µm and the crystallinity of the layer drastically changed exhibiting increased peak intensities of anatase and rutile crystal phases in comparison to untreated Ti (Fig. 5). In this context, studies have reported that a TiO_2 film composed of an anatase crystal phase can attract calcium and phosphate ions from the physiological environment to form a hydroxyapatite-like coating. It was already reported that such a coating can improve the osteogenic properties due to lattice match and superposition of hydrogen bonding grounds in anatase crystal phases. Similarly, a rutile TiO_2 film on titanium was already associated with acidic and basic hydroxyl groups (OH^-) which are conductive to cell adhesion and growth [52–54]. It is therefore believed that the mixture of anatase and rutile crystal phases in the coated Ti samples prepared in this work may positively influence the bioactivity of Ti by enhancing the osteogenic properties of Ti.

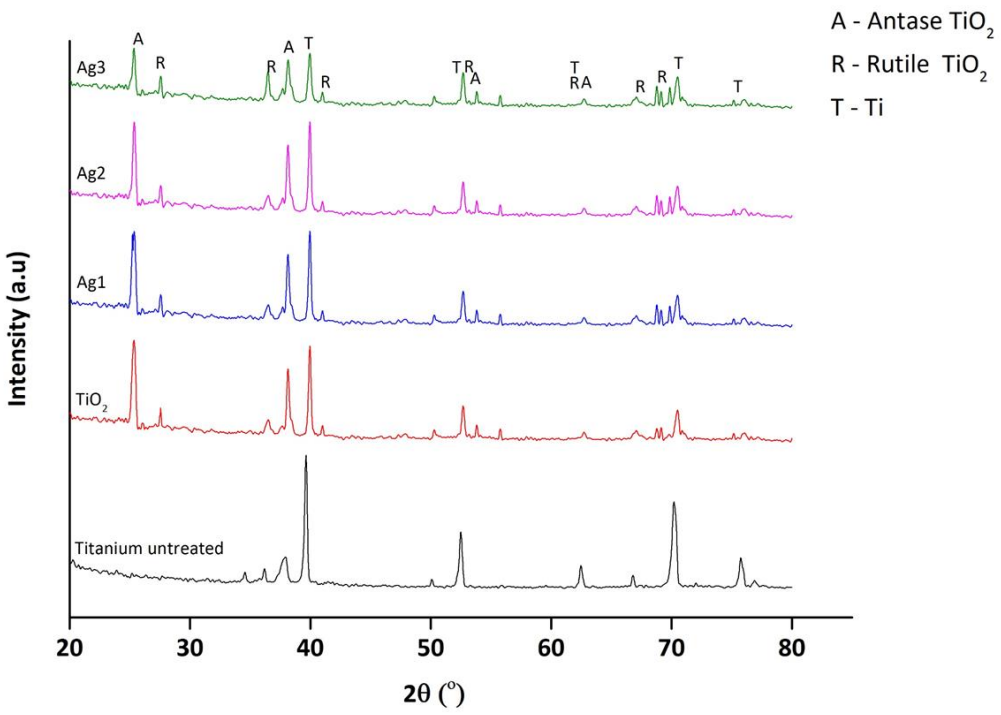

Fig. 5. XRD spectra of untreated Ti, Ag-free and Ag-doped TiO_2 coatings.

3.3 Surface wettability

Besides the surface crystallinity, surface wettability was also found to be another important aspect in improving the bioactivity of titanium surfaces. Consequently, the surface wettability of the coated Ti samples was also investigated in this work and Fig. 6(a) shows the results of this WCA analysis. The WCA value of the untreated polished Ti sample was found to be approximately 65°, while after PEO treatment, both Ag-free and Ag-doped TiO_2 samples showed a significant reduction in WCA values. In case of the Ag-free TiO_2 coating, the WCA value decreased to approximately 20°, indicating a change from a moderate to a strong hydrophilic surface. Fig. 6(a) also reveals that the presence of AgNPs on/in the porous TiO_2 coating did not result in a significant change in wettability compared to the Ag-free TiO_2 samples. The increase in wettability of the PEO treated Ti samples may therefore be primarily attributed to the transition from Ti metal to Ti oxide structures, surface crystallinity changes and surface topography variations. The latter parameter could be related to the increased porosity of the oxidized surface allowing the water droplet to better penetrate inside the pores [55].

3.4 Surface roughness

The average roughness values R_a for the untreated polished Ti, Ag-free and Ag-doped TiO_2 samples are presented in Fig.6(b). As mentioned earlier, PEO is a process that is known to increase the surface roughness of the substrate due to the in-depth growth of a porous oxide coating. The results obtained

in this work confirm this observation: the surface roughness increased from 0.11 ± 0.05 µm for the untreated polished Ti sample to 0.78 ± 0.10 µm for the Ag-free PEO treated Ti sample. Similar as in case of the surface wettability, no significant differences in surface roughness were observed between the Ag-free and Ag-doped coatings.

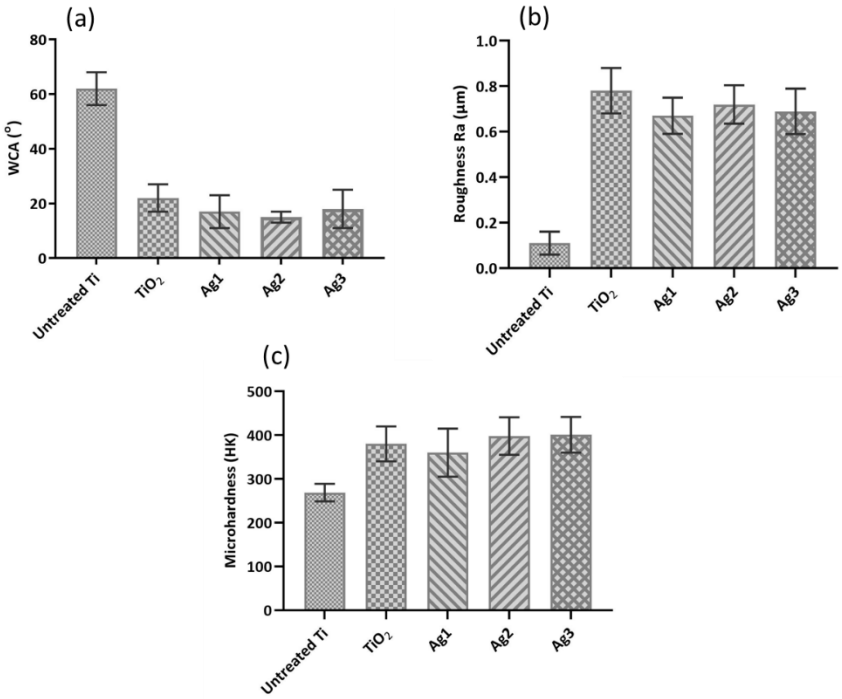

Fig. 6. WCA (a), roughness (b), microhardness (c) of untreated Ti, TiO_2, Ag1, Ag2 and Ag3

3.5 Surface microhardness

Fig. 6(c) shows the microhardness of all samples under investigation in this work using a loading force of 100 g. The microhardness of the untreated Ti substrate was found to be approximately 269 HK and after PEO treatment, the coating microhardness increased to approximately 380 HK. Again, no significant difference in surface microhardness was observed between the Ag-free and Ag-doped coatings. The increased microhardness may be caused by the presence of higher amounts of anatase and rutile phases in the PEO treated samples as microhardness is mainly depending on the structure and the phase composition. Additionally, the larger standard deviations on the PEO treated samples may also be attributed to their higher surface porosity. For clinical applications, an increase in Ti surface microhardness could be beneficial, because it increases the resistance to wear of the material, thereby positively contributing to the longevity of a Ti implant [56].

3.6 Silver ion release characteristics of the coatings

The antibacterial nature of Ag-based coatings depends on their ability to release silver ions. Studies have shown that AgNPs can provide a sustained release of sufficient Ag ions due to their high active surface area, which is not the case for Ag salts and bulk metallic forms [57]. It has already been demonstrated that AgNPs oxidize to Ag ions while interacting with an aqueous medium [58]. Hence, it is essential to quantify the amount of silver ions released from the Ag-doped TiO_2 coatings into a surrounding aqueous medium. Fig. 7(a) presents the cumulative Ag^+ release profiles of Ag-doped TiO_2 samples in distilled water for up to 7 days. This cumulative Ag^+ release is observed to parabolically increase with immersion time with different release rates, depending on the initial Ag loading. Samples with higher Ag concentration present in the coating exhibited a higher Ag^+ release at any given point during the 7 days measurement. As shown in fig. 7(b), the release of Ag^+ per day (ppb/day) was 20 ppb/day for the Ag1 sample, 78 ppb/day for the Ag2 sample and approximately 97 ppb/day for the Ag3 sample after the first immersion; this Ag^+ release eventually decreased to 9, 35 and 29 ppb/day after an immersion time of 7 days for the Ag1, Ag2 and Ag3 samples, respectively. Silver ion release profiles of the silver-doped coatings thus show a fast initial release followed by a low level of continuous release (Fig. 7(b)). While the rapid release of Ag^+ ions at the initial periods could be beneficial in preventing implant related infections after the surgical procedure, a slow release rate may contribute to a long-term antibacterial activity. In this respect, Ag^+ rates from the examined samples are higher than the reported minimum Ag^+ concentration of 0.1 ppb required to exhibit an antibacterial activity [58]. In addition, studies have also reported that Ag^+ concentrations of more than 300 ppb in human blood could cause side effects in the form of liver and kidney damage [27]. In contrast, Tweden et al. [59] reported that an Ag^+ concentration up to 1200 ppb had no cytotoxic effect on *in-vitro* fibroblast cells. Although a higher Ag content can provide an excellent antibacterial activity, it is equally important for the coating to exhibit biocompatibility. The highest cumulative silver release after 7 days in this study was 240 ppb (Ag3 sample) meaning that the Ag^+ release is well maintained below 300 ppb, which is considered the normal Ag^+ concentration in human blood [59,60].

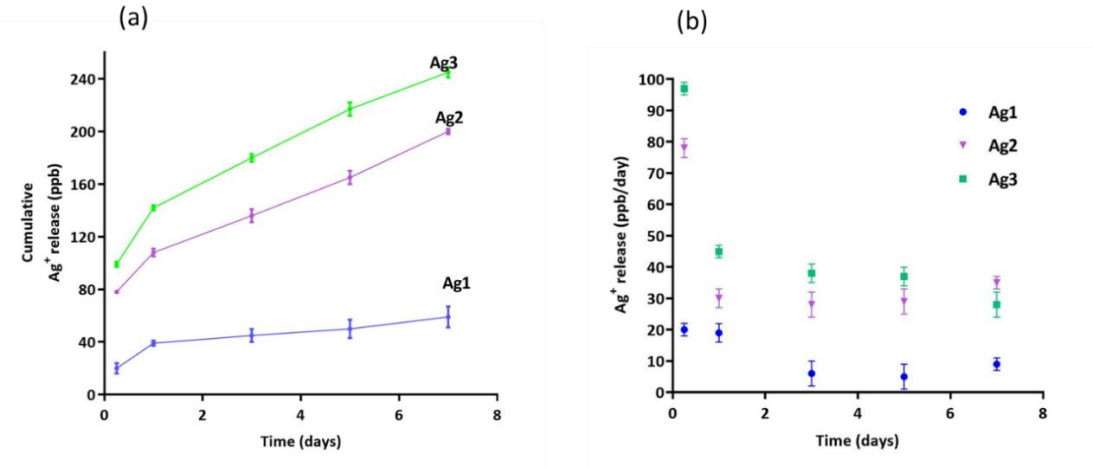

Fig. 7. Cumulative Ag^+ release (ppb) (a) and Ag^+ release rate (ppb/day) when immersed in water up to 7 days for Ag1, Ag2 and Ag3 samples.

3.7 Evaluation of the *in vitro* antibacterial activity of the coatings

The final step of this study was testing the antibacterial potential of the prepared coatings. The antibacterial activity of the coatings was investigated against *S. aureus* (Gram-positive bacterium) and *E. coli* (Gram-negative bacterium). From untreated Ti samples, approximately 10^8 CFU are recovered, both for *E. coli* and *S. aureus*. This is also reflected in the high fluorescence after staining with resazurin (Fig. 8). No reduction in *E. coli* and *S. aureus* were observed in silver-free TiO_2 coatings. In contrast, the silver-doped coatings showed a significant reduction ($p<0.05$) in cell numbers and metabolic activity. This was most pronounced for *E. coli* and for samples Ag2 and Ag3 (Fig. 8). Studies have reported that the antibacterial effect was found to be strongly dependent on the amount of AgNPs in the coatings [61], which is also observed in this work. In the case of Ag1, a 4-log reduction of *E. coli* bacteria and a 2-log reduction of *S. aureus* bacteria were observed. Samples with high silver content (Ag2, Ag3) exhibited a complete reduction of *E. coli* and a 6-log reduction of *S. aureus*. The antibacterial activity of AgNPs could be due to several mechanisms. The main mechanism suggested is the close contact of bacteria with the nanoparticles and/or release of silver ions in contact with aqueous environment [61]. Secondly, the generation of reactive oxygen species such as superoxide radicals, hydroxyl radicals, hydrogen peroxide and singlet oxygen may cause chemical damage to proteins and DNA in bacteria. Other studies demonstrated that the size and shape of the nanoparticles could also contribute to their antibacterial effects [62]. Considering the distribution of AgNPs within the TiO_2 coating, it is crucial to note that only two locations are important in exhibiting the antibacterial activity on the material, i.e Ag fused in the walls of open pores and those adherent on the surface of the oxide coating. However,

further research is needed to understand the mechanism of antibacterial activity of silver-doped TiO_2 coatings and on their *in vitro* cytotoxicity evaluation.

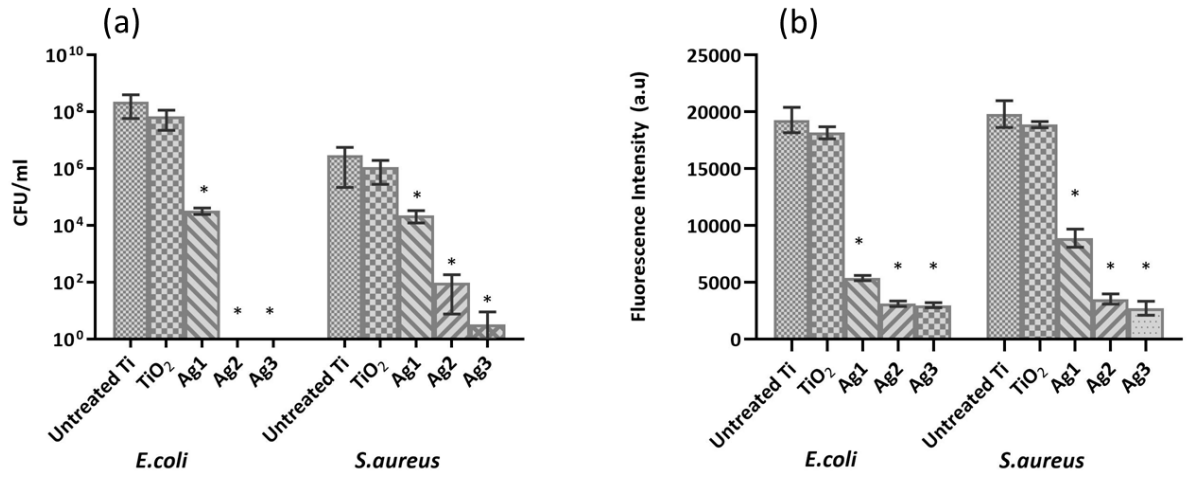

Fig. 8. Number of CFU (a) and metabolic activity (b) after 24 hours of incubation with different samples. The data are expressed as mean ± SD of 4 independent experiments (n=4). Asterisk (*) denotes significant difference at $p<0.05$ compared to the control sample (untreated Ti).

4. Conclusions

In the present study, commercially available pure titanium samples were subjected to PEO in sodium dihydrogen phosphate and sodium hydroxide containing base electrolyte with and without the addition of AgNPs (0.1 g/L, 0.5 g/L and 1g/L) at a DC voltage of 400 V for 5 min. In summary, porous TiO_2 coatings and antibacterial silver-containing TiO_2 coatings were prepared on the surface of titanium by plasma electrolytic oxidation without and with the presence of AgNPs respectively. In the latter case, AgNPs were successfully incorporated into the coating and distributed on the coating surface and inside the pores of the coating. Increasing the concentration of AgNPs in the electrolyte increased the amount of Ag in the oxidized coatings from 0.6 wt% to 3.1 wt%. In contrast, the microstructure and phase composition, surface roughness and surface wettability of the TiO_2 coatings were not affected by the incorporation of AgNPs. The silver ion release kinetics of the Ag-doped TiO_2 samples were also examined and showed a fast initial Ag^+ release followed by a slow continuous release over a period of 7 days. Additionally, the coatings synthesized in alkaline base electrolyte with added AgNPs exhibited excellent antibacterial activity against *E. coli* and *S. aureus* in comparison to the coating formed in Ag-free base electrolyte. Moreover, the antibacterial activity of the coating was found to increase with an increase in AgNPs amount in the electrolyte. The efficient bactericidal effect of the Ag-loaded coatings

can be attributed to the release of Ag^+ ions into the bacterial solution alone or in combination with contact killing.

Acknowledgements

Monica Thukkaram would like to thank the Research Foundation Flanders (FWO) for financing her PhD fellowship strategic basic research (1S13017N). Pieter Cools would like to thank the Special Research Fund (BOF) of Ghent University for financing his post-doctoral grant.

References

[1] M.A. Elias, C.N., Lima, J.H.C., Valiev, R., and Meyers, Biomedical applications of titanium and its alloys Biological Materials Science 46-49, (2008) 1–4. www.tms.org/jom.html.

[2] B.S. Necula, I. Apachitei, F.D. Tichelaar, L.E. Fratila-Apachitei, J. Duszczyk, An electron microscopical study on the growth of TiO2-Ag antibacterial coatings on Ti6Al7Nb biomedical alloy, Acta Biomater. 7 (2011) 2751–2757. doi:10.1016/j.actbio.2011.02.037.

[3] E.M. Hetrick, M.H. Schoenfisch, Reducing implant-related infections: Active release strategies, Chem. Soc. Rev. 35 (2006) 780–789. doi:10.1039/b515219b.

[4] T. Jennison, M. McNally, H. Pandit, Prevention of infection in external fixator pin sites, Acta Biomater. 10 (2014) 595–603. doi:10.1016/j.actbio.2013.09.019.

[5] H. Qu, C. Knabe, S. Radin, J. Garino, P. Ducheyne, Percutaneous external fixator pins with bactericidal micron-thin sol-gel films for the prevention of pin tract infection, Biomaterials. 62 (2015) 95–105. doi:10.1016/j.biomaterials.2015.05.041.

[6] S. Esposito, S. Leone, Prosthetic joint infections: microbiology, diagnosis, management and prevention, Int. J. Antimicrob. Agents. 32 (2008) 287–293. doi:10.1016/j.ijantimicag.2008.03.010.

[7] S.J. McConoughey, R. Howlin, J.F. Granger, M.M. Manring, J.H. Calhoun, M. Shirtliff, S. Kathju, P. Stoodley, Biofilms in periprosthetic orthopedic infections, Future Microbiol. 9 (2014) 987–1007. doi:10.2217/fmb.14.64.

[8] N. Høiby, T. Bjarnsholt, C. Moser, … G.B.-C. microbiology, undefined 2015, ESCMID guideline

for the diagnosis and treatment of biofilm infections 2014, Elsevier. (n.d.). https://www.sciencedirect.com/science/article/pii/S1198743X14000901 (accessed June 6, 2019).

[9] B.J. Nelson, M. Morra, C. Cassinelli, G. Cascardo, A. Carpi, M. Fini, G. Giavaresi, R. Giardino, A. Kozlovsky, Z. Artzi, O. Moses, N. Kamin-Belsky, R.B.-N. Greenstein, W.H. Kim, S.B. Lee, K.T. Oh, S.K. Moon, K.M.K.N. Kim, K.M.K.N. Kim, The release behavior of CHX from polymer-coated titanium surfaces, Surf. Interface Anal. 58 (2004) 1194–1200. doi:10.1002/sia.2809.

[10] A. Kozlovsky, Z. Artzi, O. Moses, N. Kamin-Belsky, R.B.-N. Greenstein, Interaction of Chlorhexidine With Smooth and Rough Types of Titanium Surfaces, J. Periodontol. 77 (2006) 1194–1200. doi:10.1902/jop.2006.050401.

[11] M. Morra, C. Cassinelli, G. Cascardo, A. Carpi, M. Fini, G. Giavaresi, R. Giardino, Adsorption of cationic antibacterial on collagen-coated titanium implant devices, Biomed. Pharmacother. 58 (2004) 418–422. doi:10.1016/j.biopha.2004.08.002.

[12] M.E. Barbour, D.J. O'Sullivan, D.C. Jagger, Chlorhexidine adsorption to anatase and rutile titanium dioxide, Colloids Surfaces A Physicochem. Eng. Asp. 307 (2007) 116–120. doi:10.1016/j.colsurfa.2007.05.010.

[13] E.I. Alarcon, K. Udekwu, M. Skog, N.L. Pacioni, K.G. Stamplecoskie, M. González-Béjar, N. Polisetti, A. Wickham, A. Richter-Dahlfors, M. Griffith, J.C. Scaiano, The biocompatibility and antibacterial properties of collagen-stabilized, photochemically prepared silver nanoparticles, Biomaterials. 33 (2012) 4947–4956. doi:10.1016/j.biomaterials.2012.03.033.

[14] Z. Jia, P. Xiu, M. Li, X. Xu, Y. Shi, Y. Cheng, S. Wei, Y. Zheng, T. Xi, H. Cai, Z. Liu, Bioinspired anchoring AgNPs onto micro-nanoporous TiO2orthopedic coatings: Trap-killing of bacteria, surface-regulated osteoblast functions and host responses, Biomaterials. 75 (2016) 203–222. doi:10.1016/j.biomaterials.2015.10.035.

[15] S. Mei, H. Wang, W. Wang, L. Tong, H. Pan, C. Ruan, Q. Ma, M. Liu, H. Yang, L. Zhang, Y. Cheng, Y. Zhang, L. Zhao, P.K. Chu, Antibacterial effects and biocompatibility of titanium surfaces with graded silver incorporation in titania nanotubes, Biomaterials. 35 (2014) 4255–4265. doi:10.1016/j.biomaterials.2014.02.005.

[16] H. Wu, X. Zhang, X. He, M. Li, X. Huang, R. Hang, B. Tang, Wear and corrosion resistance of anti-bacterial Ti-Cu-N coatings on titanium implants, Appl. Surf. Sci. 317 (2014) 614–621. doi:10.1016/j.apsusc.2014.08.163.

[17] X. Zhang, Y. Ma, N. Lin, X. Huang, R. Hang, A. Fan, B. Tang, Microstructure, antibacterial properties and wear resistance of plasma Cu-Ni surface modified titanium, Surf. Coatings Technol. 232 (2013) 515–520. doi:10.1016/j.surfcoat.2013.06.012.

[18] X. Zhang, X. Huang, L. Jiang, Y. Ma, A. Fan, B. Tang, Surface microstructures and antimicrobial properties of copper plasma alloyed stainless steel, Appl. Surf. Sci. 258 (2011) 1399–1404. doi:10.1016/j.apsusc.2011.09.091.

[19] G. Jin, H. Qin, H. Cao, S. Qian, Y. Zhao, X. Peng, X. Zhang, X. Liu, P.K. Chu, Synergistic effects of dual Zn/Ag ion implantation in osteogenic activity and antibacterial ability of titanium, Biomaterials. 35 (2014) 7699–7713. doi:10.1016/j.biomaterials.2014.05.074.

[20] G. Jin, H. Qin, H. Cao, Y. Qiao, Y. Zhao, X. Peng, X. Zhang, X. Liu, P.K. Chu, Zn/Ag micro-galvanic couples formed on titanium and osseointegration effects in the presence of S.aureus, Biomaterials. 65 (2015) 22–31. doi:10.1016/j.biomaterials.2015.06.040.

[21] K. Huo, X. Zhang, H. Wang, L. Zhao, X. Liu, P.K. Chu, Osteogenic activity and antibacterial effects on titanium surfaces modified with Zn-incorporated nanotube arrays, Biomaterials. 34 (2013) 3467–3478. doi:10.1016/j.biomaterials.2013.01.071.

[22] R. Dastjerdi, M. Montazer, A review on the application of inorganic nano-structured materials in the modification of textiles: Focus on anti-microbial properties, Colloids Surfaces B Biointerfaces. 79 (2010) 5–18. doi:10.1016/j.colsurfb.2010.03.029.

[23] M.J. Hajipour, K.M. Fromm, A. Akbar Ashkarran, D. Jimenez de Aberasturi, I.R. de Larramendi, T. Rojo, V. Serpooshan, W.J. Parak, M. Mahmoudi, Antibacterial properties of nanoparticles, Trends Biotechnol. 30 (2012) 499–511. doi:10.1016/j.tibtech.2012.06.004.

[24] S.L. Percival, P.G. Bowler, D. Russell, Bacterial resistance to silver in wound care, J. Hosp. Infect. 60 (2005) 1–7. doi:10.1016/j.jhin.2004.11.014.

[25] X. He, X. Zhang, X. Wang, L. Qin, Review of Antibacterial Activity of Titanium-Based Implants' Surfaces Fabricated by Micro-Arc Oxidation, Coatings. 7 (2017) 45. doi:10.3390/coatings7030045.

[26] M. Bosetti, A. Massè, E. Tobin, M. Cannas, Silver coated materials for external fixation devices: In vitro biocompatibility and genotoxicity, Biomaterials. 23 (2002) 887–892. doi:10.1016/S0142-9612(01)00198-3.

[27] J. Hardes, H. Ahrens, C. Gebert, A. Streitbuerger, H. Buerger, M. Erren, A. Gunsel, C. Wedemeyer, G. Saxler, W. Winkelmann, G. Gosheger, Lack of toxicological side-effects in

silver-coated megaprostheses in humans, Biomaterials. 28 (2007) 2869–2875. doi:10.1016/j.biomaterials.2007.02.033.

[28] J. Mungkalasiri, L. Bedel, F. Emieux, J. Doré, F.N.R. Renaud, F. Maury, DLI-CVD of TiO2-Cu antibacterial thin films: Growth and characterization, Surf. Coatings Technol. 204 (2009) 887–892. doi:10.1016/j.surfcoat.2009.07.015.

[29] Y.Z. Wan, G.Y. Xiong, H. Liang, S. Raman, F. He, Y. Huang, Modification of medical metals by ion implantation of copper, Appl. Surf. Sci. 253 (2007) 9426–9429. doi:10.1016/j.apsusc.2007.06.031.

[30] H. Cao, Y. Qiao, X. Liu, T. Lu, T. Cui, F. Meng, P.K. Chu, Electron storage mediated dark antibacterial action of bound silver nanoparticles: Smaller is not always better, Acta Biomater. 9 (2013) 5100–5110. doi:10.1016/j.actbio.2012.10.017.

[31] F. Meng, Z. Sun, Applied Surface Science A mechanism for enhanced hydrophilicity of silver nanoparticles modified TiO 2 thin films deposited by RF magnetron sputtering, Water. 255 (2009) 6715–6720. doi:10.1016/j.apsusc.2009.02.076.

[32] X.B. Tian, Z.M. Wang, S.Q. Yang, Z.J. Luo, R.K.Y. Fu, P.K. Chu, Antibacterial copper-containing titanium nitride films produced by dual magnetron sputtering, Surf. Coatings Technol. 201 (2007) 8606–8609. doi:10.1016/j.surfcoat.2006.09.322.

[33] B.S. Necula, J.P.T.M. Van Leeuwen, L.E. Fratila-Apachitei, S.A.J. Zaat, I. Apachitei, J. Duszczyk, In vitro cytotoxicity evaluation of porous TiO2-Ag antibacterial coatings for human fetal osteoblasts, Acta Biomater. 8 (2012) 4191–4197. doi:10.1016/j.actbio.2012.07.005.

[34] Z. Huan, L.E. Fratila-Apachitei, I. Apachitei, J. Duszczyk, Characterization of Porous TiO2 Surfaces Formed on 316L Stainless Steel by Plasma Electrolytic Oxidation for Stent Applications, J. Funct. Biomater. 3 (2012) 349–360. doi:10.3390/jfb3020349.

[35] A.L. Yerokhin, X. Nie, A. Leyland, A. Matthews, Characterisation of oxide films produced by plasma electrolytic oxidation of a Ti–6Al–4V alloy, Surf. Coatings Technol. 130 (2000) 195–206. doi:10.1016/S0257-8972(00)00719-2.

[36] M. Echeverry-Rendon, V. Duque, D. Quintero, S.M. Robledo, M.C. Harmsen, F. Echeverria, Improved corrosion resistance of commercially pure magnesium after its modification by plasma electrolytic oxidation with organic additives, J. Biomater. Appl. 33 (2018) 725–740. doi:10.1177/0885328218809911.

[37] K. Rokosz, T. Hryniewicz, S. Raaen, P. Chapon, F. Prima, Development of copper-enriched

porous coatings on ternary Ti-Nb-Zr alloy by plasma electrolytic oxidation, Int. J. Adv. Manuf. Technol. 89 (2017) 2953–2965. doi:10.1007/s00170-016-9206-z.

[38] K. Rokosz, T. Hryniewicz, P. Chapon, S. Raaen, H.R.Z. Sandim, XPS and GDOES characterization of porous coating enriched with copper and calcium obtained on tantalum via plasma electrolytic oxidation, J. Spectrosc. 2016 (2016). doi:10.1155/2016/7093071.

[39] F. Jaspard-mecuson, Aluminium plasma electrolytic oxidation (PEO) : Process investigation and growth mechanisms ., (2006) 14–18.

[40] A.B. Rogov, Plasma electrolytic oxidation of A1050 aluminium alloy in homogeneous silicate-alkaline electrolytes with edta4-complexes of Fe, Co, Ni, Cu, la and Ba under alternating polarization conditions, Mater. Chem. Phys. 167 (2015) 136–144. doi:10.1016/j.matchemphys.2015.10.020.

[41] K. Rokosz, T. Hryniewicz, Characteristics of porous biocompatible coatings obtained on Niobium and Titanium-Niobium-Zirconium (TNZ) alloy by Plasma Electrolytic Oxidation, Mechanik. (2015) 978/15-978/18. doi:10.17814/mechanik.2015.12.530.

[42] Y.T. Sul, B.S. Kang, C. Johansson, H.S. Um, C.J. Park, T. Albrektsson, The roles of surface chemistry and topography in the strength and rate of osseointegration of titanium implants in bone, J. Biomed. Mater. Res. - Part A. 89 (2009) 942–950. doi:10.1002/jbm.a.32041.

[43] D. Wei, Y. Zhou, C. Yang, Structure, cell response and biomimetic apatite induction of gradient TiO2-based/nano-scale hydrophilic amorphous titanium oxide containing Ca composite coatings before and after crystallization, Colloids Surfaces B Biointerfaces. 74 (2009) 230–237. doi:10.1016/j.colsurfb.2009.07.025.

[44] L. Zhao, H. Wang, K. Huo, L. Cui, W. Zhang, H. Ni, Y. Zhang, Z. Wu, P.K. Chu, Antibacterial nano-structured titania coating incorporated with silver nanoparticles, Biomaterials. 32 (2011) 5706–5716. doi:10.1016/j.biomaterials.2011.04.040.

[45] O. Akhavan, Lasting antibacterial activities of Ag-TiO2/Ag/a-TiO2nanocomposite thin film photocatalysts under solar light irradiation, J. Colloid Interface Sci. 336 (2009) 117–124. doi:10.1016/j.jcis.2009.03.018.

[46] L. Zhang, J. Guo, X. Huang, Y. Zhang, Y. Han, The dual function of Cu-doped TiO_2 coatings on titanium for application in percutaneous implants, J. Mater. Chem. B. 4 (2016) 3788–3800. doi:10.1039/C6TB00563B.

[47] X. Zhang, J. Li, X. Wang, Y. Wang, R. Hang, X. Huang, B. Tang, P.K. Chu, Effects of copper

nanoparticles in porous TiO2 coatings on bacterial resistance and cytocompatibility of osteoblasts and endothelial cells, Mater. Sci. Eng. C. 82 (2018) 110–120. doi:10.1016/j.msec.2017.08.061.

[48] K.M. Lee, K.R. Shin, S. Namgung, B. Yoo, D.H. Shin, Electrochemical response of ZrO2-incorporated oxide layer on AZ91 Mg alloy processed by plasma electrolytic oxidation, Surf. Coatings Technol. 205 (2011) 3779–3784. doi:10.1016/j.surfcoat.2011.01.033.

[49] X. Lu, C. Blawert, M.L. Zheludkevich, K.U. Kainer, Insights into plasma electrolytic oxidation treatment with particle addition, Corros. Sci. 101 (2015) 201–207. doi:10.1016/j.corsci.2015.09.016.

[50] E. Matykina, R. Arrabal, P. Skeldon, G.E. Thompson, Transmission electron microscopy of coatings formed by plasma electrolytic oxidation of titanium, Acta Biomater. 5 (2009) 1356–1366. doi:10.1016/j.actbio.2008.10.007.

[51] K. Rokosz, T. Hryniewicz, D. Matỳsek, S. Raaen, J. Valíček, Ł. Dudek, M. Harničárová, SEM, EDS and XPS analysis of the coatings obtained on titanium after plasma electrolytic oxidation in electrolytes containing copper nitrate, Materials (Basel). 9 (2016) 9–16. doi:10.3390/ma9050318.

[52] G. Wang, J. Li, K. Lv, W. Zhang, X. Ding, G. Yang, X. Liu, X. Jiang, Surface thermal oxidation on titanium implants to enhance osteogenic activity and in vivo osseointegration, Sci. Rep. 6 (2016) 1–13. doi:10.1038/srep31769.

[53] J.E. Collazos-Castro, A.M. Cruz, M. Carballo-Vila, M. Lira-Cantú, L. Abad, Á.P. del Pino, J. Fraxedas, A.S. Juan, C. Fonseca, A.P. Pêgo, N. Casañ-Pastor, Thin solid films., Elsevier, n.d. https://www.academia.edu/14229076/Neural_cell_growth_on_TiO2_anatase_nanostructured_surfaces (accessed June 4, 2019).

[54] H.-K. Tsou, P.-Y. Hsieh, M.-H. Chi, C.-J. Chung, J.-L. He, Improved osteoblast compatibility of medical-grade polyetheretherketone using arc ionplated rutile/anatase titanium dioxide films for spinal implants, J Biomed Mater Res Part A. 100 (2012) 2787–2792. doi:10.1002/jbm.a.34215.

[55] J. Bico, U. Thiele, D. Quéré, Wetting of textured surfaces, Colloids Surfaces A Physicochem. Eng. Asp. 206 (2002) 41–46. doi:10.1016/S0927-7757(02)00061-4.

[56] P. Soares, A. Mikowski, C.M. Lepienski, E. Santos, G.A. Soares, V. Swinka Filho, N.K. Kuromoto, Hardness and elastic modulus of TiO2 anodic films measured by instrumented indentation, J.

Biomed. Mater. Res. - Part B Appl. Biomater. 84 (2008) 524–530. doi:10.1002/jbm.b.30900.

[57] K.N.J. Stevens, O. Crespo-Biel, E.E.M. van den Bosch, A.A. Dias, M.L.W. Knetsch, Y.B.J. Aldenhoff, F.H. van der Veen, J.G. Maessen, E.E. Stobberingh, L.H. Koole, The relationship between the antimicrobial effect of catheter coatings containing silver nanoparticles and the coagulation of contacting blood, Biomaterials. 30 (2009) 3682–3690. doi:10.1016/j.biomaterials.2009.03.054.

[58] R. Kumar, H. Münstedt, Silver ion release from antimicrobial polyamide/silver composites, Biomaterials. 26 (2005) 2081–2088. doi:10.1016/j.biomaterials.2004.05.030.

[59] K. Tweden, J. Cameron, … A.R.-T.J. of heart, undefined 1997, Biocompatibility of silver-modified polyester for antimicrobial protection of prosthetic valves., Europepmc.Org. (n.d.). https://europepmc.org/abstract/med/9330181 (accessed June 4, 2019).

[60] A. de la R. Brutel, … K.D.-T.J. of heart, undefined 2000, First clinical experience with a mechanical valve with silver coating., Europepmc.Org. (n.d.). https://europepmc.org/abstract/med/10678384 (accessed June 4, 2019).

[61] M. Rai, A. Yadav, A. Gade, Silver nanoparticles as a new generation of antimicrobials, Biotechnol. Adv. 27 (2009) 76–83. doi:10.1016/j.biotechadv.2008.09.002.

[62] J.R. Morones, J.L. Elechiguerra, A. Camacho, K. Holt, J.B. Kouri, J.T. Ramírez, M.J. Yacaman, The bactericidal effect of silver nanoparticles, Nanotechnology. 16 (2005) 2346–2353. doi:10.1088/0957-4484/16/10/059.